

Vortex Penetration In Magneto-Superconducting Heterostructures.

Serkan Erdin

School of Physics & Astronomy, University of Minnesota,
116 Church St. S.E., Minneapolis, MN 55455

We report our results on vortex penetration in two realizations of heterogeneous magneto-superconducting systems (HMSS) based on London approach; semi-infinite ferromagnetic (FM)-superconducting (SC) bilayers and a FM dot on a semi-infinite SC film. In the first case, we study quantitatively the vortex entry in FM-SC bilayers which manifests Bean-Livingston-like vortex barrier, controlled by FM film's magnetization and SC film's Ginzburg parameter. In the second case, we investigate the conditions for spontaneous vortex creation and determine the position of vortex for various values of magnetization and the dot's position.

PACS Number(s): 74.25.Dw, 74.25.Ha, 74.25.Qt, 74.78.-w

Heterogeneous magneto-superconducting systems (HMSS) are made of ferromagnetic (FM) and superconducting (SC) pieces separated by thin layers of insulating oxides. In contrast to the case of a homogeneous ferromagnetic superconductor studied during the last two decades, the two order parameters, the magnetization and the SC electron density do not suppress each other [1,2]. In HMSS, the strong interaction between FM and SC components stems from the magnetic fields generated by the inhomogeneous magnetization and the supercurrents as well as SC vortices. Strong interaction of the FM and SC systems not only gives rise to a new class of novel phenomena and physical effects, but also shows the important technological promise of devices whose transport properties can be easily tuned by comparatively weak magnetic fields.

Various theoretical realizations of HMSS have been proposed by different groups, such as arrays of magnetic dots on the top of a SC film [1,3], ferromagnetic/superconducting bilayers (FSB) [4], and magnetic nanorods embedded into a superconductor [5], whereas only sub-micron magnetic dots covered by thin SC films have been prepared and studied [6,8]. The experimental samples of FM-SC hybrid systems were prepared by means of electron beam lithography and lift-off techniques [9]. Both in-plane and out-of-plane magnetization was experimentally studied. The dots with magnetization parallel to the plane were fabricated from Co, Ni, Fe, Gd-Co and Sm-Co alloys. For the dots with magnetization perpendicular to the plane which requires high anisotropy along hard-axis, Co/Pt multilayers were used [10].

In the most of theoretical studies, SC subsystem is considered to be infinite size for the sake of computational simplicity. To this date, there has not been an analytical analysis of boundary and edge effects in FM-SC heterostructures, though vortex entry conditions in

type II superconductors are previously studied [11-13]. However, from both experimental and theoretical point of view, finite or semi-infinite systems are more interesting and realistic, and their study offers better understanding of vortex matter in HMSS. A author also believes that analytical and quantitative study of aforementioned systems will shed light on solving other open problems pertaining to HMSS. For example, we earlier predicted that in a finite temperature interval below the SC transition the FSB is unstable with respect to SC vortex formation in FM-SC bilayers (FSB) [14]. The slow decay ($\propto 1/r$) of the long-range interactions between Pearl vortices makes the structure that consists of alternating domains with opposite magnetization and vorticity energetically favorable. It is possible that the long domain nucleation time can interfere with the observation of described textures. We also expect that domain nucleation starts near the edge, which makes qualitative study of edges in aforementioned systems necessary. Quantitative study of this dynamic process is still in progress. For this purpose, and having been motivated by current interest in HMSS, in this work, we attempt to study vortex entry conditions in HMSS. To our purpose, we work with a method based on London-Maxwell equations, which is fully explained elsewhere [15]. London approach works well for large Ginzburg ($\kappa = \kappa_{eff} = \lambda/d \gg 1$) parameter, where $\kappa_{eff} = \lambda/d$ is the effective penetration depth [16], and λ is coherence length. Indeed, for thin SC films, Ginzburg parameter is on order of 50-100. Previously, our method was introduced for vortex structures in infinite films. Here, we extend it to semi-infinite systems. To this end, we benefit from Kogan's work on a Pearl vortex near the edge of SC thin film in which SC piece's size is considered to be semi-infinite [17]. Likewise, we consider FM subsystems on semi-infinite SC and FM systems in which, we assume that magnetization points perpendicular to the FM film's plane.

In this work, we first consider semi-infinite SC and FM films and study vortex entry barrier. Our calculations show that there exists Bean-Livingston-like surface barrier [18] for the vortices created by FM film. Next, we consider a circular magnetic dot near the film's edge and investigate the conditions for vortices to appear and their configurations. It turns out that, in contrast to the infinite systems, vortices are not trapped right at the dots center, but they are shifted slightly from the center to the SC film's edge or opposite direction, depending on the dot's magnetization, position and size. Physics behind this effect is simple. In the semi-infinite system, vortex interacts with both its image vortex and the magnetic dot. The competition between these two attractions determines vortex's position. The outline of this article is as follows: in the first section, we introduce the method to study edge effects in FM-SC systems. In the next section, we apply our method based on Maxwell-London equations to two different cases; semi-infinite FM-SC bilayers and FM dot on a semi-infinite SC film. We conclude with results and discussions.

I. METHOD

Finite and semi-infinite systems are not as easy and straightforward as infinite systems, and they usually require more careful treatment due to the boundary of the systems. Earlier, Kogan developed a clever technique based on London approach to study a vortex near the 2d film's edge [17]. While developing our method, we stick to his technique and geometry in which a very thin SC film is located at x-y halfplane while its edge is at x=0 (see Fig.1), and generalize his method for more than one vortex. We also assume that no vortex is closer to the SC film's edge than coherence length, because London theory does fail in the vicinity of .

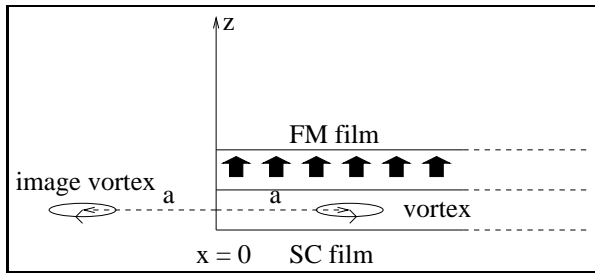


FIG. 1. Semi-infinite FM-SC bilayer.

$$h_z + \frac{4}{c} \int_{x^0 > 0}^Z d^2 r^0 \frac{r^2 G(r^0)}{R} + \int_1^Z dy^0 \frac{\partial_{x^0} G(r^0)}{R} \Big|_{x^0=0} + 4 \int_1^Z r^2 G(r) = \frac{4}{c} \int_0^X n_j(r - r_j) - 4 \int_0^Z (r - g_m)_z : \quad (6)$$

Solving the above equation in halfplane is difficult. However, this difficulty can be removed by solving (6) in the Fourier space and using the boundary conditions. That is, at the film's edge (x = 0), the normal component

We start with London equation for the vortices with vorticity n_j located at r_j ,

$$h + \frac{4}{c} \int_{x^0 > 0}^Z d^2 r^0 \frac{r^2 G(r^0)}{R} = \frac{4}{c} \int_0^X n_j(r - r_j); \quad (1)$$

where j_s is supercurrent density in the SC subsystem. In the presence of FM subsystem which is also considered to be very thin and located at x-y halfplane as SC subpiece, Eq.(1) turns to

$$h + \frac{4}{c} \int_{x^0 > 0}^Z d^2 r^0 \frac{r^2 G(r^0)}{R} = \frac{4}{c} \int_0^X n_j(r - r_j) + \frac{4}{c} \int_0^Z dy^0 \frac{\partial_{x^0} G(r^0)}{R} \Big|_{x^0=0}; \quad (2)$$

where $j = j_s + j_n$ and $j_n = cr \times m$. Averaging Eq.(2) over the thickness of SC film, one finds

$$h_z + \frac{4}{c} \int_{x^0 > 0}^Z d^2 r^0 \frac{r^2 G(r^0)}{R} = \frac{4}{c} \int_0^Z dy^0 \frac{\partial_{x^0} G(r^0)}{R} \Big|_{x^0=0} + \frac{4}{c} \int_0^X n_j(r - r_j); \quad (3)$$

where g is the 2-d current density, which can be calculated by solving Eq.(3) together with the Biot-Savart integralequation and the continuity equation $\nabla \cdot g = 0$. In terms of the surface current, the Biot-Savart equation is given by

$$h_z = \frac{1}{c} \int_{x^0 > 0}^Z d^2 r^0 \frac{r^2 G(r^0)}{R} - R^3; \quad (4)$$

where $R = r - r^0$. Defining the surface current density in terms of a scalar function $G(r)$ as $g = \nabla \times G(r) \hat{z}$, using $R^3 = r^0(1/R)$ and integrating Eq.(4) by parts, one can obtain

$$h_z = \frac{1}{c} \int_{x^0 > 0}^Z d^2 r^0 \frac{r^2 G(r^0)}{R} + \int_1^Z dy^0 \frac{\partial_{x^0} G(r^0)}{R} \Big|_{x^0=0}; \quad (5)$$

where the first term gives the contribution from the entire surface current distribution whereas the second term is the contribution from the film's edge. The direct substitution of Eq.(5) into Eq.(2) gives

$$h_z + \frac{4}{c} \int_{x^0 > 0}^Z d^2 r^0 \frac{r^2 G(r^0)}{R} + \int_1^Z dy^0 \frac{\partial_{x^0} G(r^0)}{R} \Big|_{x^0=0} + 4 \int_1^Z r^2 G(r) = \frac{4}{c} \int_0^X n_j(r - r_j) - 4 \int_0^Z (r - g_m)_z : \quad (6)$$

of current density is zero, namely $g_x(0; y) = 0$, whereas, at infinity the current distribution vanishes. This implies that the scalar function is constant at the film's boundaries. For simplicity, it can be set to zero. To have G

vanish at the edge, we set $G(x; y) = G(x; y)$. The Fourier transform of Eq.(6) reads

$$\int_0^Z dx^0 e^{ik_x x^0} (\partial_{x^0}^2 - k_y^2) G(x^0; k_y) + \int_0^Z dy^0 [\partial_{x^0} G(x^0)]_{k^0=0} e^{ik_y y^0} + 2k^3 G(k) = i \frac{c_0}{k} \sum_j n_j e^{ik_y y_j} \sin(k_x x_j) - 2k (i\tilde{K} - g_{m;k_x}) z; \quad (7)$$

where $k = (k_x; k_y)$. Replacing x^0 by x^0 and writing the Eq.(7) for k_x , one obtains

$$\int_0^Z dx^0 e^{ik_x x^0} (\partial_{x^0}^2 - k_y^2) G(x^0; k_y) + \int_0^Z dy^0 [\partial_{x^0} G(x^0)]_{k^0=0} e^{ik_y y^0} + 2k^3 G(k) = i \frac{c_0}{k} \sum_j n_j e^{ik_y y_j} \sin(k_x x_j) - 2k (i\tilde{K} - g_{m;k_x}) z; \quad (8)$$

where $\tilde{K} = (k_x; k_y)$. Subtracting (8) from (7), the vortex and magnetic parts of the scalar function are found as

$$G_v(k) = \frac{2c_0}{i} \sum_j n_j \frac{e^{ik_y y_j} \sin(k_x x_j)}{k(1+4k)}; \quad (9)$$

$$G_m(k) = 2i \frac{[k - g_{m;k_x} \tilde{K} - g_{m;k_x} z]}{k(1+4k)}; \quad (10)$$

Taking the inverse Fourier transform of Eq.(9), the vortex contribution in real space is found as

$$G_v(r) = \frac{c_0}{2} \sum_j n_j \int_0^Z \frac{(J_0(k\tilde{r} - r_j) - J_0(k\tilde{r} + r_j))}{1+4k} dk; \quad (11)$$

Note that the first term in (11) represents the j^{th} vortex located at $r_j = (x_j; y_j)$, whereas the second term is the contribution of j^{th} image vortex, or antivortex, at $\tilde{r}_j = (-x_j; y_j)$. Next, we calculate the 2-d current density. Keeping in mind that it is discontinuous at the \ln 's edge, the Fourier components of the current density read

$$A(r) = \frac{n_0}{4} \left[\frac{4}{\tilde{r} - a_j} - \frac{4}{\tilde{r} + a_j} + \frac{4}{2} Y_1 \left(\frac{\tilde{r} - a_j}{4} \right) + H_1 \left(\frac{\tilde{r} - a_j}{4} \right) - Y_1 \left(\frac{\tilde{r} + a_j}{4} \right) + H_1 \left(\frac{\tilde{r} + a_j}{4} \right) \right]; \quad (15)$$

where H and Y are the Struve and the second kind Bessel functions. At short distances ($r \ll \lambda$), A behaves as $(n_0/16) [(1+4/C=2 \ln 2=2) (\tilde{r} - a_j - \tilde{r} + a_j) + \tilde{r} - a_j \ln(\tilde{r} - a_j/4) - \tilde{r} + a_j \ln(\tilde{r} + a_j/4)]$ whereas, at large distances, it decays slowly in space, namely $(n_0/8) (1 - \tilde{r} - a_j - 1 - \tilde{r} + a_j)$. $C = 0.577...$ is Euler constant. Magnetic field due to vortex in z direction

$$h_z(r) = \frac{n_0}{4} \left[\frac{1}{\tilde{r} - a_j} - \frac{1}{\tilde{r} + a_j} - \frac{1}{8} H_0 \left(\frac{\tilde{r} - a_j}{4} \right) - Y_0 \left(\frac{\tilde{r} - a_j}{4} \right) - H_0 \left(\frac{\tilde{r} + a_j}{4} \right) - Y_0 \left(\frac{\tilde{r} + a_j}{4} \right) \right]; \quad (17)$$

$$g(x > 0; y) = \frac{d^2 k}{(2\pi)^2} (ik - \tilde{z}) G(k) e^{ik \cdot r};$$

$$g(x < 0; y) = 0; \quad (12)$$

Using Eq.(12), one can compute vector potential and the magnetic field through

$$A = \frac{4}{c} \frac{g}{Q^2}; \quad h = \frac{4}{ic} \frac{g}{Q^2} Q; \quad (13)$$

where $Q = k + k_z \hat{z}$. Taking the inverse Fourier of Eq.(13), vector potential is found as

$$A(r) = \frac{c_0}{2} \sum_j n_j \int_0^Z \frac{(J_1(k\tilde{r} - r_j) - J_1(k\tilde{r} + r_j)) e^{k \cdot \tilde{r}_j}}{1+4k} dk; \quad (14)$$

At the SC \ln 's surface ($z = 0$), vector potential for one vortex with vorticity n , located at $r = a$ reads

reads

$$h_z(r) = \frac{n_0}{8} \int_0^Z \frac{(J_0(k\tilde{r} - a) - J_0(k\tilde{r} + a)) k e^{k \cdot \tilde{r}}}{1+4k} dk \quad (16)$$

At $z = 0$, magnetic field reads

$$Y_0 \left(\frac{\tilde{r} - a_j}{4} \right) - H_0 \left(\frac{\tilde{r} + a_j}{4} \right) - Y_0 \left(\frac{\tilde{r} + a_j}{4} \right) : \quad (17)$$

The asymptotics of the magnetic field at small and large distances are

$$h_z = \frac{n_0}{4} \frac{1}{r-a} - \frac{1}{r+a} + \frac{1}{4} \ln \frac{r-a}{r+a} \quad r < a \quad (18)$$

$$h_z = \frac{4n_0}{r^3} \frac{1}{r-a} - \frac{1}{r+a} \quad r \gg a \quad (19)$$

The total energy of FM-SC system reads

$$E = E_v + E_{vm} + E_m; \quad (20)$$

$$E_v = \sum_i \frac{n_i^2}{16} \ln \frac{8}{e^c} - \frac{1}{2} \sum_i \frac{x_i}{2} + \sum_{i>j} X$$

where $\phi_0(x) = Y_0(x) - H_0(x)$. Vortex-magnetization interaction energy is calculated as in [15]:

$$E_{vm} = \frac{1}{16} \int_0^Z r' \left(\frac{1}{2} \int_0^Z m \phi_0^2 dx \right) dx; \quad (23)$$

where integration is performed over the half space. Note that we take $\epsilon = 50$ in our numerical calculations.

A. Semi-Infinite FM-SC Bilayers

In this part, we study a semi-infinite FM film on top of a semi-infinite SC film. Both films are taken to be very thin, lie on x-y half plane whereas their edges are located at $x = 0$ (see Fig.1). We assume that FM film has uniform magnetization along z direction and has high anisotropy, so that its magnetization does not change direction due to magnetic field of vortex. The magnetization of FM film reads

$$m = m_0 \hat{z}; \quad (24)$$

Magnetic current in real space and Fourier space is given as

$$g_m = m_0 \hat{z} \delta(x); \quad g_{m,k} = 2 m_0 \hat{z} \delta(k_x) \delta(k_y); \quad (25)$$

Substituting Eq.(24) into Eq.(10), one can find the scalar potential as

$$G_m(k) = \frac{8 m_0 c}{k} \frac{k_x \delta(k_y)}{(1 + 4 k^2)}; \quad (26)$$

Taking the inverse Fourier transform of Eq.(26), we find

$$G_m(x) = \frac{m_0 c}{4} f \left(\frac{x}{a} \right); \quad (27)$$

where $f(x) = \int_0^{\infty} dk_x \sin(k_x x) = (1 + k_x^2)$. The asymptotics of $f(x)$ are

where E_v is the vortex energy, E_{vm} is the interaction of vortex and magnetic subsystem and finally E_m is self-energy of magnetic subsystem, which will be ignored at further calculations, since it is inappropriate for our problem. Vortex energy is calculated by Kogan [17] as

$$E_v = \sum_{i,j}^{P_0} \frac{n_i n_j}{2c} G_v(r_i - r_j); \quad (21)$$

where P_0 denotes the restricted sum in which only $i = j$ and $i > j$ are taken into account. Eq.(21) leads to

$$E_v = \sum_{i,j} n_i n_j \left(\frac{r_i - r_j}{4} + \frac{r_i + r_j}{4} \right); \quad (22)$$

$$f(x) = \frac{1}{2} + x(\ln(x) + C) \quad x < 1; \quad (28)$$

$$f(x) = \frac{1}{x}; \quad x > 1;$$

Using Eq.(12) and Eq.(13), z component of the screened magnetic field at $z = 0$ due to FM film, reads

$$h_z(r) = \frac{m_0}{4} \int_0^Z \frac{k_x \sin(k_x \frac{x}{4})}{1 + k_x^2} dk_x; \quad (29)$$

The magnetic field decays as $1/x$ for $x < a$ and $1/x^2$ for $x > a$. In order to study vortex configuration, we need to calculate total effective energy of the system. To this end, we consider a simple case, namely a vortex with a single flux located at $r = a$. For this case, vortex energy for a single vortex reads (see Eq.(22))

$$E_v = \frac{1}{16} \ln \frac{8}{e} - \frac{1}{2} \ln \frac{a}{2}; \quad (30)$$

whereas the vortex-magnetization interaction energy can be calculated by means of Eq.(23).

$$E_{vm} = m_0 \int_0^{\infty} \frac{2}{4} f \left(\frac{a}{x} \right) dx; \quad (31)$$

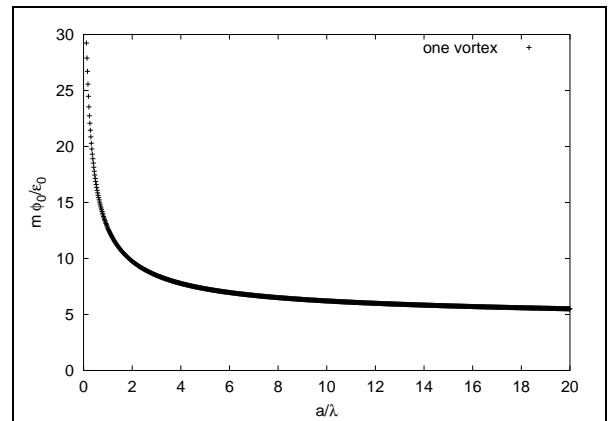


FIG. 2. Phase diagram of a single vortex created by semi-infinite FM film. In the region below curve, vortex does not appear, whereas it becomes energetically favorable in area above the curve.

The sum of Eq.(22) and Eq.(31) gives the effective total energy of the system. Vortex becomes energetically favorable when effective total energy becomes less than zero. Equating the effective energy to zero, one can obtain the curve for spontaneous creation of vortex. This curve,

$$\frac{m_0}{\mu_0} = \frac{\ln\left(\frac{8}{e}\right) - \frac{1}{2} \left(H_0\left(\frac{a}{2}\right) - Y_0\left(\frac{a}{2}\right) \right)}{1 - \frac{2}{\pi} f\left(\frac{a}{4}\right)} \quad (32)$$

separates the regions where the vortex appears spontaneously and does appear as seen in Fig.2. For large values of m_0/μ_0 ratio, the vortex comes out near the edge. On the other hand, it prefers going further away from the surface for small ratio of m_0/μ_0 . We can estimate the minimum value of magnetization of FM film through effective energy for infinite films [15], which is $E_{eff} = \mu_0 \ln(\frac{8}{e}) - m_0$. Equating this equation to zero and solving it for m , we find $m_{c1} = \mu_0(16^{-2} \ln(\frac{8}{e}))$. When magnetization exceeds this value, the vortex appears very far away from the edge. In order to get vortex appear close to the edge, m must be significantly larger than m_{c1} . Another interesting thing is that the system manifests Bean-like surface barrier for the vortex. The surface barrier is controlled by m_0/μ_0 and Ginzburg parameter κ . We analyze three regimes for this ratio for fixed $\kappa = 1$. When $m < m_{c1}$, vortex does not appear (see Fig.3). In the second regime, $m_{c1} < m < m_{c2}$, vortex prefers going further away from the surface, whereas, when $m > m_{c2}$, the barrier disappears (see Fig.4). m_{c2} is the second critical magnetization, at which barrier disappears, and can be calculated through the condition that the slope $\partial E_{tot}/\partial x|_{x=0}$ is zero, which gives $m_0/\mu_0 = 2 \ln(4)$. When ratio m_0/μ_0 is greater than this, the barrier disappears. Physically, two contributions play an important role for the vortex barrier. Namely, the vortex is attracted to SC film's edge through its attraction towards image vortex whereas it is repelled by FM film's edge. Competition between these two factors controls the barrier.

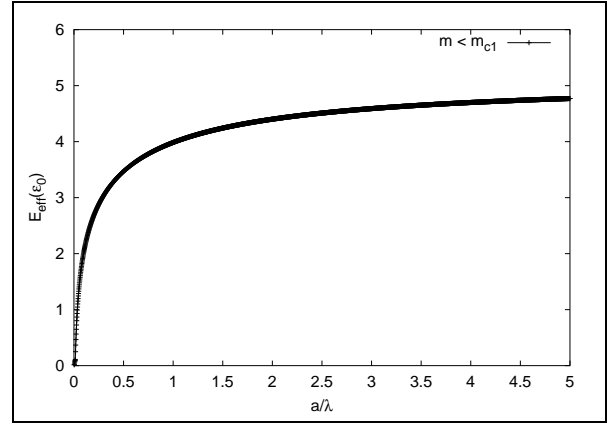


FIG. 3. The effective energy versus the vortex's position. When $m < m_{c1}$, vortex does not appear.

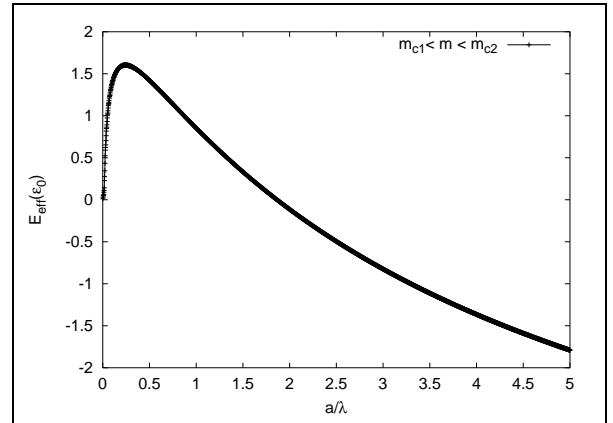


FIG. 4. The effective energy versus the vortex's position. When $m_{c1} < m < m_{c2}$, the surface barrier shrinks toward the edge of SC film, and vortex is created little further from the edge.

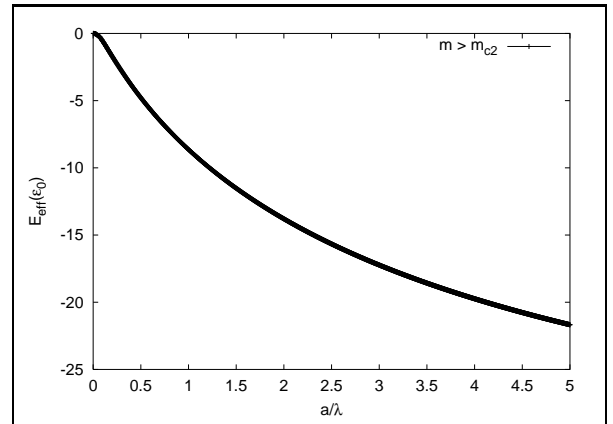


FIG. 5. The effective energy versus the vortex's position. When $m > m_{c2}$ barrier disappears, and vortex can be seen anywhere in SC film.

In this case, we study a circular FM disc on top of semi-infinite SC film. Earlier, we studied the conditions for the vortex states to appear on a similar system, in which SC film, however was infinite. Due to the circular symmetry of FM dot, vortex was appearing at the dot's center. In this section, we study the vortex states in more realistic case and investigate the role of edge effects on the spontaneous formation of vortex due to FM dot. To this end, we start with the magnetization of a circular

$$h_z(r; z) = 4\pi R \int_0^{\infty} \frac{J_1(kR) [J_0(kr - r_d) - J_0(kr + r_d)] k^2 e^{kz}}{1 + 4k} dk: \quad (35)$$

Outside the dot, magnetic field decays rapidly in space, namely, for $r < r_d$, $h \sim r^3$, whereas for $r > r_d$, $h \sim r^{-5}$.

$$E_{vm} = -4\pi R \int_0^{\infty} J_1(kR) \frac{[J_0(kr_d - a) - J_0(kr_d + a)]}{1 + 4k} dk: \quad (36)$$

After we formulate the total effective energy as $E = E_v + E_{vm}$, where E_v is given in Eq.(30), we study the conditions for a vortex to appear spontaneously. The criteria for spontaneous vortex formation is that effective energy becomes negative. However, vortex in semi-infinite system also interacts with its image. Therefore, it is necessary to minimize total effective energy with respect to the vortex position. To this end, we first fix the dot's location and value of $m_0 = 0$ and vary the vortex's position afterwards, to find the minimum total effective energy. In our calculations, we investigate where vortex

first comes out, and how it is shifted with further increase of $m_0 = 0$. For this purpose, we determine vortex's position for different values of the $r_d = 1, R = 1$ and $m_0 = 0$, by optimizing the total effective energy. Our results are shown in Table I and Fig.6.

According to our calculations, vortex appears first close to the edge except $r_d = R = 10$ case, in which it sits at the dot's center. On the other hand, when $m_0 = 0$ is increased further, vortex is first shifted towards the dot's center. With further increase of $m_0 = 0$, it drifts away from the dot's center. However, this is not always general picture. In the case of $r_d = R = 5, 3$, vortex is located at the dot's center even for large values of $m_0 = 0$. However, for larger dot's sizes ($r_d = R = 1$ and $r_d = 2$)

FM disc located at $r_d = (x_d; 0)$,

$$m = m_0 (R - |r - r_d|)(z)z; \quad (33)$$

where R is the radius of circular dot. The Fourier transform of Eq.(33) reads

$$m_k = 2\pi R \frac{J_1(kR) e^{ikx_d}}{k}: \quad (34)$$

Using Eq. (10,12,13) together with Eq.(34), one can calculate the screened magnetic field due to FM dot as

From Eq.(23), the vortex-magnetic disc interaction energy reads

vortex first appears away from the dot's center. This situation differs from the vortex in infinite system. In the latter, only force acting on vortex stems from the vortex-magnetization interaction, and due to the dot's circular symmetry, it comes out at the dot's center. However, in this case, there is another force coming from vortex-image vortex, which decays slowly $h \sim r$ for large distances $r > r_d$ and pulls vortex towards the SC film's edge, whereas the force exerted by the magnetic dot pushes vortex towards the dot's center. As a result, vortex's position is determined by the balance between these two forces.

TABLE I. The position of vortices for different values of the $r_d = 1, R = 1$ and $m_0 = 0$. The two columns on the left are input.

$r_d =$	$R =$	$a =$	$m_0 = 0$
2.0	2.0	2.04	17
2.0	2.0	2.32	187
3.0	3.0	3.12	31
3.0	3.0	3.44	132
4.0	4.0	4.20	11
4.0	4.0	4.56	185

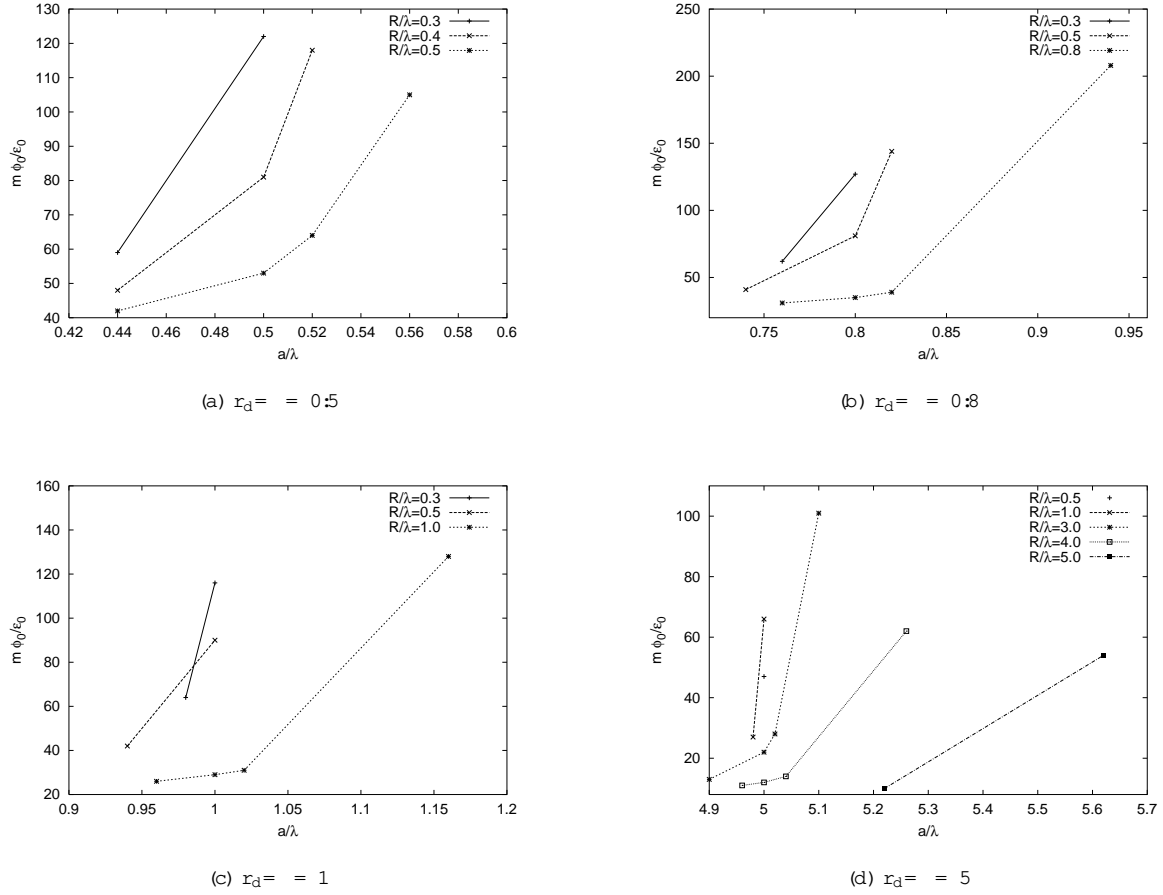


FIG. 6. Position of vortex a/λ versus $m\phi_0/\epsilon_0$ for various locations r_d and sizes R/λ of magnetic dot.

II. CONCLUSIONS

In this article, we studied vortex entry conditions in HMSS. First, we generalized Kogan's method for quantitative study of semi-infinite HMSS. For applications, we first considered semi-infinite FM film on top of semi-infinite SC film. The quantitative analysis of this system showed that the vortex undergoes Bean-like barrier which is controlled by two intrinsic properties of system; FM film's magnetization m and Ginzburg parameter λ . Note that our result is valid only for a single flux. Our study for the case of several vortices will be published elsewhere. Secondly, we studied a single circular FM dot on a semi-infinite SC film. We analyzed the conditions for spontaneous vortex creation and vortex location for various positions of the dot. It turns out that the vortex does not always appear at the dot's center, which differs from the case in which similar dot on an infinite SC film. In closing, there are two important contributions in semi-infinite HMSS; attraction of vortex to the edge through its image vortex and vortex-magnetization interaction. As a result of competition between these two factors, pec-

uliar physical effects which do not come out in infinite HMSS, appear. In this work, we studied the simplest cases to get idea about edge effects in HMSS. However, there are still several interesting realizations that can be studied via the method that is developed here. We leave them for possible future works.

-
- [1] I.F. Lyuksyutov and V.L. Pokrovsky, Phys. Rev. Lett. 81, 2344 (1998).
 - [2] I.F. Lyuksyutov and V.L. Pokrovsky, in Superconducting Superlattices II: Native and Artificial, edited by Ivan Bozovic and Davor Pavuna, SPIE Proceedings Vol. 3480 (SPIE-International Society for Optical Engineering, Bellingham, WA, 1998), p. 230.
 - [3] S. Erdin, Physica C 391, 140 (2003).
 - [4] I.F. Lyuksyutov and V.L. Pokrovsky, cond-mat/9903312.
 - [5] I.F. Lyuksyutov and D.G. Naugle, Modern Phys. Lett. B 13, 491 (1999).

- [6] J.I. Martin, M. Velez, J. Nogues and I.K. Schuller, Phys. Rev. Lett. 79, 1929 (1997).
- [7] D.J. Morgan and J.B. Ketterson Phys. Rev. Lett. 80, 3614 (1998).
- [8] Y. O tani, B. Pannetier, J.P. Nozieres and D. G ivord, J. Magn. Mag. Mat. 126, 622 (1993).
- [9] M. J. Van Bael, K. Tem st, V.V. Moshchalkov and Y. Bruynseraede, Phys. Rev. B 59, 14674 (1999).
- [10] M. J. Bael, L. Van Look, K. Tem st et al. Physica C 332, 12 (2000).
- [11] P.G. de Gennes, Sol. St. Com m . 3, 127 (1965).
- [12] L. K ram er, Phys. Rev. 170, 475 (1968).
- [13] D. Y. Vodolazov, I.L. Maksim ov and E.H. Brandt, Physica C 384, 211 (2003).
- [14] S.Erdin, I.F. Lyuksyutov, V.L. Pokrovsky and V.M. Vinokur, Phys. Rev. Lett. 88, 017001 (2002).
- [15] S. Erdin, A.M. Kayali, I.F. Lyuksyutov, and V.L. Pokrovsky, Phys. Rev. B 66, 014414 (2002).
- [16] A.A. Abrikosov, Introduction to the Theory of Metals (North Holland, Amsterdam, 1986).
- [17] V.G. Kogan, Phys. Rev. B 49, 15874 (1994).
- [18] C.P. Bean and J.D. Livingstone, Phys. Rev. Lett. 12, 14 (1964).